Thermoresponsive Luminescent Electrospun Fibers Prepared From Poly(DMAEMA-co-SA-co-StFl) Multifunctional Random Copolymers

ARTICLE *in* ACS APPLIED MATERIALS & INTERFACES · OCTOBER 2010

Impact Factor: 6.72 · DOI: 10.1021/am100760a · Source: PubMed

4 AUTHORS, INCLUDING:

Yu-Cheng Chiu
Stanford University
39 PUBLICATIONS **240** CITATIONS
SEE PROFILE

Chi-Ching Kuo
National Taipei University of Technology
24 PUBLICATIONS **456** CITATIONS
SEE PROFILE

Wen-Chang Chen
National Taiwan University
274 PUBLICATIONS **6,912** CITATIONS
SEE PROFILE

ARTICLE

Thermoresponsive Luminescent Electrospun Fibers Prepared From Poly(DMAEMA-*co*-SA-*co*-StFl) Multifunctional Random Copolymers

Yu-Cheng Chiu,[†] Chi-Ching Kuo,[‡] Jung-Ching Hsu,[†] and Wen-Chang Chen*[,†,‡]

Department of Chemical Engineering and Institute of Polymer Science and Engineering, National Taiwan University, Taipei 106, Taiwan

ABSTRACT We report novel thermoresponsive electrospun (ES) fibers prepared from multifunctional random copolymers of poly((2-(dimethylamino)ethyl methacrylate)-*co*-(stearyl acrylate) -*co*-(9,9-dihexyl-2-(4-vinylpenyl)-9H-fluorene)) (poly(DMAEMA-*co*-SA-*co*-StFl)). The moieties of DMAEMA, SA, and StFl were designed to exhibit the thermoresponsive, physical cross-linking, and fluorescent functionality, respectively. The effects of the copolymer compositions on the morphology and photoluminescence of the prepared ES fibers were explored. The prepared **P4** copolymer with the DMAEMA/SA/StFl mole ratio of 92/3/5 showed the lower critical solution temperature (LCST) of 32.5 °C. A significant temperature-dependent swelling and de-swelling behavior was found in the **P4** ES fibers, which had the diameter of 753 ± 174 nm and 5−10 nm StFl aggregated domain. Accompanied with volume-changing on the **P4** ES fibers, a reversible photoluminescence (PL) quenching was also observed during the heating and cooling cycle between 40 and 60 °C. Such reversible switching of the "on−off" PL intensity was probably due to the light absorption ability of the StFl moiety, resulted from the extended/compact structural transformation on the PDMAEMA moiety. Furthermore, the high surface/volume ratio of the ES fibers led a much better temperature response compared with the corresponding spin-coated film. The present study demonstrated that the ES fibers prepared from multifunctional copolymers exhibited the thermoreversible variation on both volume and photoluminescence intensity.

KEYWORDS: electrospinning fibers • thermoresponsive • copolymers • physically cross-linking • luminescence • sensing

INTRODUCTION

Multifunctional copolymers containing π-conjugated rod and the environmental-stimulus coil have attracted extensive scientific interest for sensory device applications because their morphology and photophysical properties could be significantly tuned by external stimuli, such as pH, temperature, light, etc. (1−18). Poly(*N*-isopropylacrylamide) (PNIPAAm) (19, 20) and poly(2-(dimethylamino)ethyl methacrylate) (PDMAEMA) (21−23) are widely studied thermoresponsive polymers. They exhibit a hydrophilic extended structure below their lower critical solution temperature (LCST), whereas above the LCST, they dehydrate and form a compact structure. We are particularly interested in PDMAEMA-based copolymers because they show both thermal and pH responsive characteristics for multifunctional sensory devices (13, 19, 20, 24−28). For example (28), a water pH-responsive molecular brush of polythiophene-graft-PFMAEMA was developed on the basis of the conformation change at different pH values. In our recent report (13), the micellar aggregate of PF-*b*-PDMAEMA in water exhibited a reversible change of surface structure from cylinder-bundles to spheres over a heating-cooling cycle and the LCST decreased with increasing pH. The PL intensity of PF-*b*-PDMAEMA in water was thermoreversible on the basis of its LCST, behaving as an on/off fluorescence indicator of temperature or pH.

Electrospinning (ES) has emerged as a new technique to produce various functional fibers because it has the advantages of low cost, flexible morphology tuning, and high-throughput continuous production (29−39). The high surface/volume ratio of the ES fibers attracted extensive studies for sensory applications (35−37, 40−45). In addition, the aggregate morphology and photophysical properties of the π-conjugated rod-containing ES fibers were efficiently tuned through different environmental stimuli. For example, PF-*b*-PNIPAAm/PMMA blend ES fibers showed both reversible thermoresponsive luminescence characteristics and wettability, which were superior to the spin-coated films (40). Recently, Okuzaki and his coworkers (46) demonstrated that the poly((*N*-isopropylacrylamide)-*co*-(stearyl acrylate)) (poly(NIPAAm-*co*-SA)) ES fibers exhibited reversible and fast volume changes by changing temperature. The physical cross-linked SA moiety prevented the dissolution of the ES fibers in water. It would be of interest to explore the SA-based thermoresponsive luminescent ES fibers using the π-conjugated rod-containing copolymers.

In this study, we report the synthesis and characterization of new thermoresponsive copolymers, poly((2-(dimethylamino)ethyl methacrylate)-*co*-(stearyl acrylate)-*co*-(9,9-dihexyl-2-(4-vinylpenyl)-9H-fluorene) (poly(DMAEMA-*co*-SA-*co*-StFl). Different copolymer ratios of poly(DMAEMA-*co*-SA-

* Author to whom all correspondence should be addressed. Tel: 886-2-23628398. Fax: 886-2-23623040. E-mail: chenwc@ntu.edu.tw.
Received for review August 18, 2010 and accepted October 4, 2010
[†] Department of Chemical Engineering, National Taiwan University.
[‡] Institute of Polymer Science and Engineering, National Taiwan University.
DOI: 10.1021/am100760a

Published on Web 10/21/2010

Scheme 1. Synthesis of Poly(DMAEMA-*co*-SA-*co*-StFl), P1−P4

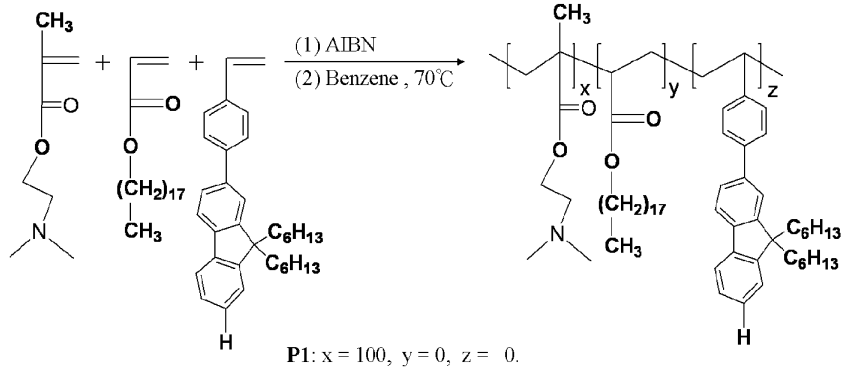

P1: x = 100, y = 0, z = 0.
P2: x = 87, y = 0, z = 13.
P3: x = 95, y = 0, z = 5.
P4: x = 92, y = 3, z = 5.

Table 1. Polymerization Conditions, Molecular Weights, and Properties of Poly(DMAEMA-*co*-SA-*co*-StFl), P1−P4

polymer	composition[a] DMAEMA:SA:StFl	M_n[b]	PDI[b]	T_d (°C)	T_g (°C)	LCST (°C)
P1	100:0:0	23 610	1.52	288	14	40.0
P2	87:0:13	28 510	2.07	317	43	[c]
P3	95:0:5	26 690	2.32	309	17	34.0
P4	92:3:5	25 690	1.92	321	23	32.5

[a] Molar ratio (%), estimated from ^{1}H NMR. [b] Determined by GPC with THF eluent. [c] Insoluble in water at room temperature.

co-StFl) were synthesized by free radical copolymerization, as shown in Scheme 1 and Table 1. ES fibers of poly(DMAEMA-*co*-SA-*co*-StFl) were prepared by a single-capillary spinneret. The fiber morphologies were characterized by field-emission scanning electron microscope (FE-SEM), laser confocal microscope (Confocal), and transmission electron microscopy (TEM). The photophysical properties were studied by steady-state photoluminescence (PL) with the temperature varied from 40 to 60 °C. The new multifunctional ES fibers exhibited both thermoreversible luminescence and swelling/deswelling characteristics, which were much more sensitive than those of spin-coated films.

EXPERIMENTAL SECTION

Materials. Stearyl acrylate (SA), obtained from Polysciences, Inc., was recrystallized from ethanol solution. 2-(Dimethylamino)ethyl methacrylate (DMAEMA) (Acros, 99%), was passed through the Al_2O_3 column prior to polymerization. 9,9-Dihexyl-2-(4-vinylphenyl)-9H-fluorene (StFl) was prepared according to our previous report (47). Azobisisobutyronitrile (AIBN) (Acros, 99%) was recrystallized from ethanol solution. Chloroform (CF) and benzene (HPLC grade, ECHO) were used as received.

General Procedures of Polymerization. Poly(DMAEMA-*co*-SA-*co*-StFl) was synthesized by free radical copolymerization of the following three monomers, DMAEMA, SA, and StF1, as shown in Scheme 1. Poly(DMAEMA-*co*-SA-*co*-StFl) with different monomer ratios were denoted **P1**−**P4**, as listed in Table 1. The concentration of AIBN used as the initiator was 0.007 M. Reaction mixture containing benzene and monomers was degassed by bubbling nitrogen for 30 min first and then reacted at 70 °C for 16 h. In the following, the reaction mixture was poured into hexane, precipitated, filtered, and dried at room temperature under a vacuum to get the polymer.

Synthesis of P1. A reaction mixture of 2080.5 mg (13.3 mmol) of DMAEMA, 8.2 mg (0.05 mmol) of AIBN, and 7 mL of benzene was used to afford a white solid (yield: 62%. ^{1}H NMR (CD_2Cl_2), δ (ppm): 0.87−1.03 (3H, $-CH_2C(C\underline{H}_3)-$), 1.78−1.90 (2H, $-C\underline{H}_2C(CH_3)-$), 2.53(2H, $-OCH_2C\underline{H}_2N(CH_3)_2$), and 4.03 (2H, $-OC\underline{H}_2CH_2N(CH_3)_2$). Number-averaged molecular weight (M_n) and polydispersity index (PDI) estimated from GPC are 23 610 and 1.52, respectively.

Synthesis of P2. A reaction mixture of 1965.1 mg (12.5 mmol) of DMAEMA, 963.2 mg (2.2 mmol) of the StFl, 8.2 mg (0.05 mmol) of AIBN, and 7 mL of benzene was used to afford a white solid (yield:66%). ^{1}H NMR (CD_2Cl_2), δ (ppm): 0.75−1.41 (25H, $-CH_2C(C\underline{H}_3)-$, $Ar-(CH_2(C\underline{H}_2)_4C\underline{H}_3))_2$), 1.84−2.03 (8H, $-C\underline{H}_2C(CH_3)-$,$-(CH_3)CC\underline{H}_2CH-$, $Ar-(C\underline{H}_2(CH_2)_4CH_3))_2$), 2.27 (6H, $-N(C\underline{H}_3)_2$), 2.54 (2H, $-OCH_2C\underline{H}_2N(CH_3)_2$), 4.03 (2H, $-OC\underline{H}_2CH_2N(CH_3)_2$), and 7.16−7.71 (11H, phenyl group and fluorene aromatic protons). Number-averaged molecular weight (M_n) and polydispersity index (PDI) estimated from GPC are 28 510 and 2.07, respectively.

Synthesis of P3. A reaction mixture of 1971.3 mg (12.6 mmol) of DMAEMA, 288.2 mg (0.7 mmol) of the StFl, 8.2 mg (0.05 mmol) of AIBN, and 7 mL of benzene was used to afford a white solid (yield:61%). ^{1}H NMR (CD_2Cl_2), δ (ppm): 0.78-1.40 (25H, $-CH_2C(C\underline{H}_3)-$ $Ar-(CH_2(C\underline{H}_2)_4C\underline{H}_3))_2$), 1.81−2.09 (8H, $-C\underline{H}_2C(CH_3)-$,$-(CH_3)CC\underline{H}_2CH-$, $Ar-(C\underline{H}_2(CH_2)_4CH_3))_2$), 2.25 (6H, $-N(C\underline{H}_3)_2$), 2.53 (2H, $-OCH_2C\underline{H}_2N(CH_3)_2$), 4.03 (2H, $-OC\underline{H}_2CH_2N(CH_3)_2$), 7.16−7.74 (11H, phenyl group, and fluorene aromatic protons). Number-averaged molecular weight (M_n) and polydispersity index (PDI) estimated from GPC are 26 690 and 2.32, respectively.

Synthesis of P4. A reaction mixture of 1867.54 mg (11.9 mmol) of DMAEMA, 214.3 mg (0.7 mmol) of the SA, 288.2 mg (0.7 mmol) of the StFl, 8.2 mg (0.05 mmol) of AIBN, and 7 mL of benzene was used to afford a white solid (Yield:56%). ^{1}H NMR (CD_2Cl_2), δ (ppm): 0.77−1.27 (58H, $-CH_2C(C\underline{H}_3)-$, $-OCH_2CH_2(C\underline{H}_2)_{15}C\underline{H}_3$, $Ar-(CH_2(C\underline{H}_2)_4C\underline{H}_3))_2$), 1.81−2.06 (8H, $-C\underline{H}_2C(CH_3)-$,$-(CH_3)CC\underline{H}_2CH-$, $Ar-(C\underline{H}_2(CH_2)_4CH_3))_2$), 2.25 (6H, $-N(C\underline{H}_3)_2$), 2.53 (2H, $-OCH_2C\underline{H}_2N(CH_3)_2$), 4.03 (4H, $-OC\underline{H}_2CH_2N(CH_3)_2$, $-OC\underline{H}_2(CH_2)_{16}CH_3$), 7.16−7.74 (11H, phenyl group, and fluorene aromatic protons). Number-averaged molecular weight (M_n) and polydispersity index (PDI) estimated from GPC are 25 690 and 1.92, respectively.

Electrospun Fibers and Spin-Coated Thin Films. Poly(DMAEMA-*co*-SA-*co*-StFl) was dissolved in chloroform with the concentration of 150 mg/mL for preparing the ES fibers. To enhance the conductivity of electrospun solution, we added

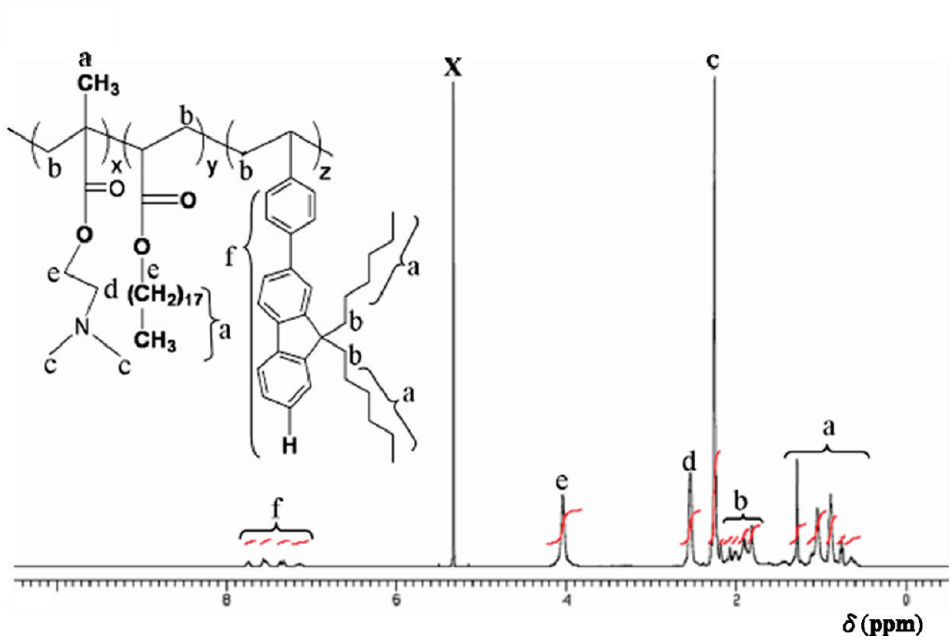

FIGURE 1. ^{1}H NMR spectrum of P4 in CD_2Cl_2.

benzyl triethylammonium chloride (BTEAC, a soluble organic salt) of 5 wt % (with respect to the polymer). A single-capillary spinneret ES device was employed to produce the ES fibers, similar to our previous report (33). The polymer solution was fed into the metallic needle by syringe pumps (KD Scientific model 100, USA), with the feed rate of 0.8−1.0 mL/h. The tip of the metallic needle was connected to a high-voltage power supply (Chargemaster CH30P SIMCO, USA), and a piece of aluminum foil or quartz was placed 15 cm below the tip of the needle to collect ES fibers. The spinning voltage was maintained at 13−15 KV during whole ES process. All experiments were carried out at room temperature and relative humidity of about 50%.

For the comparison with properties of the ES fibers, the corresponding polymer thin films were spin-coated on glass substrate from the same polymer solutions at a spin rate of 1000 rpm for 60 s.

Characterization. ^{1}H nuclear magnetic resonance (NMR) data was recorded at room temperature on a Bruker AV 500 MHz spectrometer using the residual proton resonance of the deuterated dichloromethane. Gel permeation chromatographic analysis was performed on a Lab Alliance RI2000 instrument (two column, MIXED-C and D from Polymer Laboratories) connected with one refractive index detector from Schambeck SFD GmbH. All GPC analyses were performed on polymer/THF solution at the flow rate of 1 mL min^{-1} at 40 °C and calibrated with polystyrene.

Thermal analyses were carried out on a differential scanning calorimetry (DSC) from TA Instruments (TA Q100) with heating cycle from −10 to +90 °C at the heating rate of 10 °C/min and a thermalgravimetric analyzer (TGA) from Perkin-Elmer 7 with heating range from 100 to 800 °C at a heating rate of 10 °C/min. Phase transition of the prepared polymer solution was recorded by monitoring the transmittance of a 550 nm light beam on a Mini 1240 UV−visible spectrophotometer (Shimadzu). The polymer concentration in water was 0.1 wt %, and the temperature was raised from 20 to 75 °C in 1° increments every 60 min.

The morphologies of ES fibers were performed through field-emission scanning electron microscope (FE-SEM, JEOL JSM-6330F) and transmission electron microscopy (TEM, JEOL 1230). SEM samples were sputtered with platinum prior to the images characterization and analysis was operated at accelerating of 10 kV. TEM images were obtained by operating voltage at 100 keV and samples were stained with ruthenium tetroxide (RuO_4). The StFl domains were selectivity stained with RuO_4 and appeared dark, whereas the unstained PDMAEMA and PSA domains appeared light in TEM images. Fluorescence optical microscope images were taken using Two Photon Laser Confocal Microscope (Leica LCS SP5).

The samples of the ES fibers and spin-coated films for photoluminescence spectra at different temperatures were prepared as described below: ES fibers and spin-coated films were heated by water between 40 to 60 °C for 1 h to reach equilibrium state. The samples were then put in a vacuum oven for 6 h and the corresponding temperature to remove water. Fluorescence (PL) spectra were measured later to study photophysical properties. All photoluminescence spectra of the ES fibers and spin-coated films were also recorded on Fluorolog-3 spectrofluorometer (Horiba Jobin Yvon) excited at the wavelength of 290 nm, as described in our previous study (33−37).

RESULTS AND DISCUSSION

Characterization of Poly(DMAEMA-*co*-SA-*co*-StFl). Figure 1 shows the ^{1}H NMR spectrum of **P4** with the DMAEMA/SA/StFl mole ratio of 92/3/5 in CD_2Cl_2. The chemical structures of the other three polymers, **P1**−**P3**, are shown in Figure S1 of the Supporting Information. The proton peak X in Figure 1 is d-dichloromethane. The proton signals of the phenyl group and fluorene aromatic ring on the StFl moiety are observed at 7.16−7.74 ppm (peak f). The proton peak at 4.03 ppm (peak e) is attributed to the methylene protons on the DMAEMA or SA moiety. The peaks at 2.25 ppm (peak c) and 0.77−1.27 ppm (peak a) are assigned to the protons on the DMAEMA and alkyl side chain on StFl or SA, respectively. The peaks b and d are attributed to the protons on the alkyl chain and DMAEMA moiety, respectively. The estimated copolymer composition estimated from the peak integration is consistent with the proposed structure. It indicates the successful synthesis of the copolymers shown in scheme 1. The number-averaged M_n and PDI of **P1**, **P2**, **P3**, and **P4** are (23610, 1.52), (28510, 2.07),

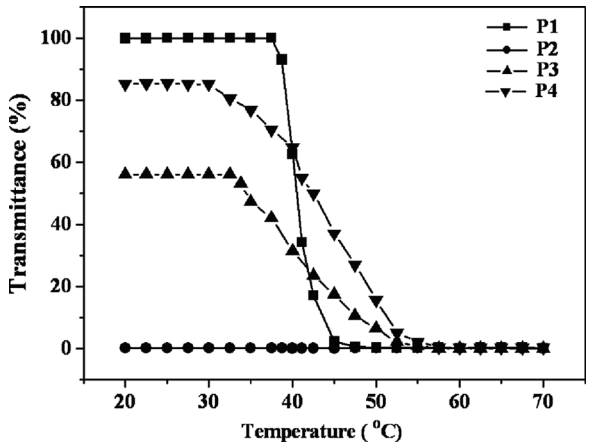

FIGURE 2. Variation of optical transmittance with temperature (20−75 °C): (a) P1 (■), (b) P2 (●), (c) P3 (▲), (d) P4 (▼).

(26690, 2.32), and (25690, 1.92), respectively. The copolymer compositions and other physical data are summarized in Table 1. Chloroform and THF are common solvents for the copolymers, whereas water is a poor solvent for the SA or StFl segments. **P1**, **P3**, and **P4** are soluble in water below its LCST, but **P2** is insoluble.

The thermal decompositions (T_d) of the copolymers (**P2**−**P4**, Figure S2 of the Supporting Information) are between 309 and 321 °C, which are higher than the PDMAEMA homopolymer (**P1**, 288 °C), as shown in Table 1. On the other hand, the glass transition temperature (T_g) of **P1**−**P4** (Figure S3 of the Supporting Information) are 14, 43, 17, and 23 °C, respectively, at the heating rate of 10 °C/min under nitrogen atmosphere. **P2**−**P4** copolymers have the higher T_g than the **P1** homopolymer due to the introduction of the rigid poly(StFl) segment (T_g = 70 °C) (47).

Figure 2 shows the typical optical transmittance (at 550 nm) vs. temperature curves of **P1**-**P4**. **P1** behaves a thermoreversible soluble-to-insoluble phase transition in the aqueous medium at around 40 °C (LCST). However, the incorporation of the hydrophobic moieties facilitates chain aggregation in the aqueous solution and lowered the LCST for **P3** (34.0 °C) and **P4** (32.5 °C). As reported in the literature (48), the LCST of PDMAEMA could be changed by copolymerization with hydrophobic and hydrophilic monomer. However, **P2** is insoluble in water because the high hydrophobic StFl content results in the significant reduction on the hydrophilic characteristic and thus no LCST characteristic was observed.

Morphology of Poly(DMAEMA-*co*-SA-*co*-StFl) ES Fibers. Figure 3 shows the SEM images of the ES fibers prepared from **P2**, **P3**, and **P4**, respectively. Note that the FE-SEM image of **P1** ES fibers with the fiber diameter of 1917±315 nm is shown in Figure S4 of the Supporting Information. The inset figure shows the enlarged FE-SEM image of the above ES fibers. Note that all of **P1**−**P4** were dissolved in chloroform with the solution concentration of 150 mg/mL by adding 5 wt % BTEAC salt for preparing the ES fibers. As shown in Figure 3(A), the **P2** ES fibers using $CHCl_3$ as the processing solvent have average diameter of 1025 ± 596 nm. The average fiber diameter was estimated

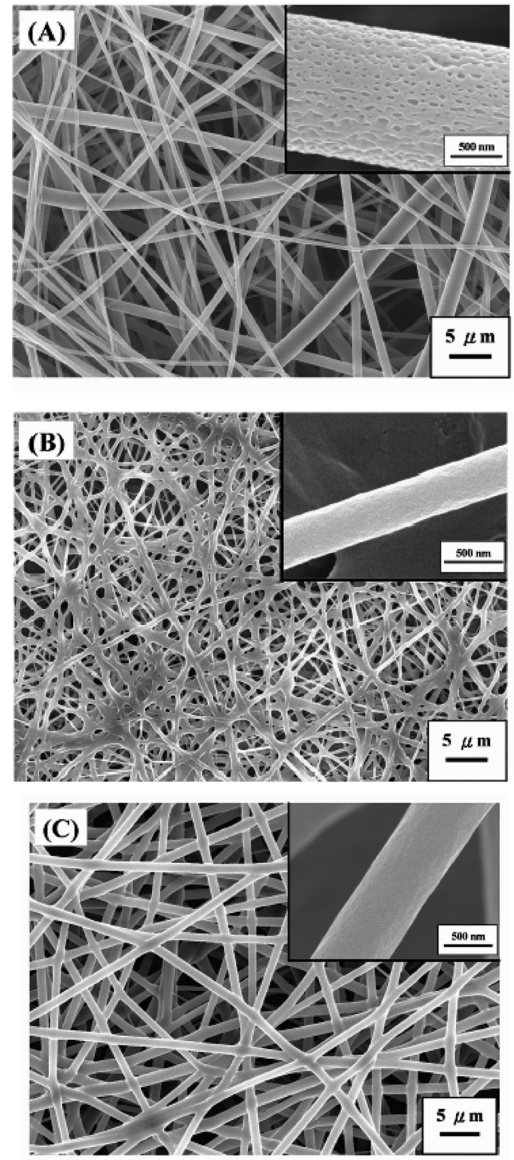

FIGURE 3. FE-SEM images of poly(DMAEMA-*co*-SA-*co*-StFl) ES fibers: (A) P2, (B) P3, and (C) P4. The inset figures show the enlarged FE-SEM images of the above ES fibers.

based on a statistical average of 50 fibers from each sample. As shown in Figure 3(A), a porous surface structure with the pore size of 50−100 nm is observed in the inset SEM image, which is mostly oriented in the axis direction. The rapid evaporation of low boiling point solvent ($CHCl_3$) and a subsequent rapid solidification during the ES process lead to the porous structure, similar to our previous study (33, 34, 36, 37). The strong stretching force associated with ES process induces orientation of these pores along the axis of a fiber. On the other hand, the **P3** and **P4** ES fibers have the average diameters of 631 ± 201 nm and 753 ± 174 nm, respectively. However, compared to the **P2** ES fibers, both of the **P3** and **P4** ES fibers exhibit nonporous and smooth surface despite preparing from the same solvent $CHCl_3$. It is probably due the higher T_g of the two copolymers, similar to those reported in the literature (49). The diameter ranges of the **P2, P3,** and **P4** ES fibers are 200−1800, 400−800, and 600−800 nm respectively. The fiber diameter range was

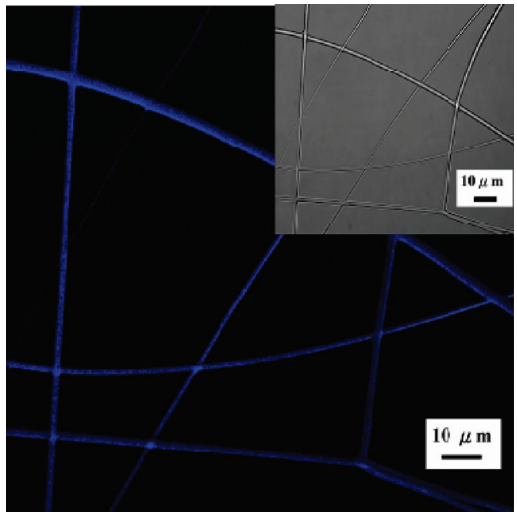

FIGURE 4. Laser confocal microscope image of the P4 ES fibers. The inset figure shows the optical image.

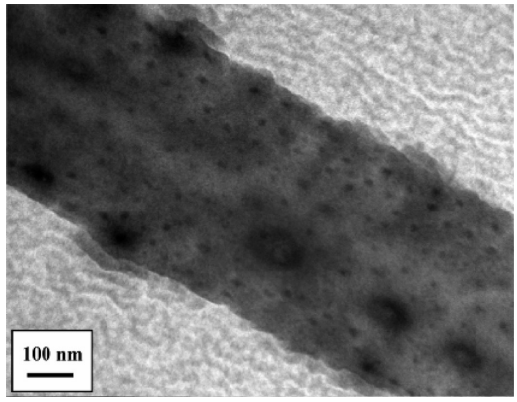

FIGURE 5. TEM micrograph of the P4 ES fibers under the dry state.

enlarged with increasing the StFl composition. The more rigid structure of the StFl moiety probably leads to an unstable cone-jet model through ES process and thus less uniform ES fibers are observed, similar to our previous report on the PFO/PMMA blend ES fibers (33).

Figure 4 shows the laser confocal and optical images of **P4** ES fibers, which emitted uniform blue-color light. It indicates the successful incorporation of the St-Fl moiety into the random copolymers. The TEM image of the **P4** ES fibers is shown in Figure 5. The dark fiber-like structure with the domain size of 5−10 nm in the TEM image is assigned to the StFl aggregated domain since it is selectivity stained with RuO_4. Note that the unstained DMAEMA and SA domains appeared light in the TEM image. Such fiber-like structure is probably attributed to the strong stretching force associated with electrospinning, similar to our previous report (33, 34, 36).

To observe the ES fibers morphology with varying temperature in pure water, the **P1**-**P4** ES fibers were collected on a small piece of aluminum foil and then immersed them in water at 40 or 60 °C, respectively. After 5 min, the samples were picked into a flask containing liquid nitrogen to solidify them instantly. Then, the residual water immediately was removed under vacuum for 30 min to retain the original morphology. Figure 6 shows the SEM images of the ES fibers prepared form the above procedures. Figure 6(A) shows the morphology of the PDMAEMA homopolymer (**P1**) ES fibers as the temperature varied from the dry state to 40 or 60 °C. As show in the figure, the **P1** fibers are dissolved by water at its LCST around 40 °C and form an irregular film. Although the **P1** ES fibers exhibit a hydrophobic characteristic at 60 °C, the fiber morphologies are slightly swelled in water due to their high surface/volume ratio. To improve the stability of those ES fibers in the water during temperature variation, the hydrophobic StFl moiety is introduced into the polymers. As shown in Figure 6(B), there is no significant structural difference (B-1, B-2, and B-3) of **P2** ES fibers at the dry state, 40 and 60 °C, respectively. In addition, it maintains a similar morphology as the dry state even in pure water at 20 °C (Figure S5 of the Supporting Information). It suggests that the highly hydrophobic StFl content significantly reduces its hydrophilic characteristic of **P2** and results in the insolubility of the copolymer in water without LCST. However, as shown in Figure 6(C), the **P3** ES fibers with a lower StFl content exhibit a slightly swelling characteristic at 40 °C but de-swelling at 60 °C. Note that pure PDMAEMA is soluble in water below 40 °C, but the above ES fibers could maintain fiber shape at 40 °C (Figure 6(C-2). It indicates that the hydrophobic StFl moiety improves the fiber structural stability but without significant thermo-responsive property. By incorporating the SA moiety with a long alkyl chain into the copolymer, the LCST of the **P4** shifts from 40 °C to around 32 °C. As the **P4** ES fibers are immersed from the dry state (Figure 6(D-1)) to pure water at 40 °C (Figure 6(D-2)), the fiber structure is significantly swollen in water due to the hydrophilic DMAEMA moiety. However, these swollen fibers still maintain their cylindrical shape and do not dissolve in water at 40 °C, due to the physical cross-linked SA moiety. On the other hand, the fiber diameter is reduced from 2.0 to 1.0 μm (Figure 6D-2 and D-3) as the temperature is increased from 40 to 60 °C. Such volume variation is due to the water expelling from the ES fibers as the temperature exceeds the LCST. The structural variation of the **P2**−**P4** ES fibers upon temperature variation would result in significant difference on the photophysical properties, as discussed in the following section.

Photoluminescence of Poly(DMAEMA-*co*-SA-*co*-StFl) ES Fibers. Figure 7(A)−(C) show the variation on the PL spectra of the **P2**-**P4** ES fibers with the temperature heating up from 40 to 60 °C. The corresponding PL spectra of the above ones through the reverse cooling process are shown in the inset figures. In the figure, the PL spectra exhibit the main emission peak around 356 nm, which is attributed to the StFl moiety (47). As shown in Figure 7(A), there is no obvious PL intensity change on the **P2** ES fibers between 40 and 60 °C because the copolymer has no LCST characteristic. However, the **P3** ES fibers with a lower StFl content exhibits a slight change on the PL intensity with varying temperature, as shown in Figure 7(B). It indicates that the copolymer with 95 mol % of the DMAEMA moiety becomes very slightly swelling or shrinking under temperature stimuli. On the other hand, a significant quenching on

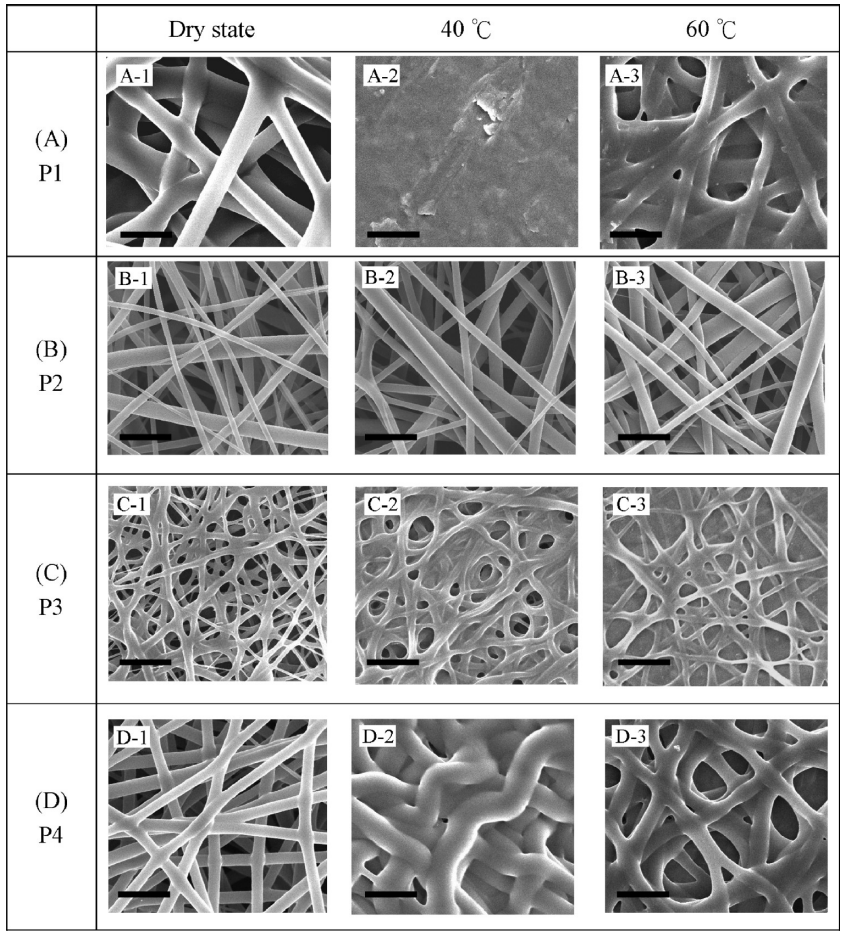

FIGURE 6. FE-SEM images of poly(DMAEMA-*co*-SA-*co*-StFl) ES fibers were treated by water as temperature variation from 40 to 60 °C: (A) P1, (B) P2, (C) P3, and (D) P4. All scale bars are 5 μm.

the PL intensity of the **P4** ES fibers is found in Figure 7(C), as the temperature is increased from 40 to 60 °C. The emission intensity is reduced upon increasing temperature and increased again by reducing temperature, due to the morphological change in Figure 6(D). However, no PL intensity change between 40 and 60 °C is found on the corresponding **P4** based thin films (Figure S6 in the Supporting Information). It indicates that the **P4** ES fibers have a much better thermoresponsive performance than the corresponding spin-coated film, because of the high surface-to-volume ratio. Furthermore, the variation in the PL intensity on the **P4** ES fibers with the heating-cooling cycle could be repeated several times (see Figure S7 in the Supporting Information), indicating its potential sensing applications.

The above thermoreversible luminescence characteristics could be explained as below. As shown in the Figure 8, the morphological change of the **P4** ES fibers soaked in water is exhibited as the temperature at 40 or 60 °C. In the case of 40 °C, the hydrophilic C═O and N−H groups in the PDMAEMA interact easily with water molecules to form intermolecular hydrogen bonding. However, the swollen ES fibers are insoluble in water due to the physically corsslinked SA segment (46, 50). When the temperature is raised to 60 °C (above the LCST), the intermolecular hydrogen bonding between the PDMAEMA and water no longer exists, leading to the release water molecules from the fibers. Besides, the conformation of PDMAEMA is collapsed and densely packed that may suppress the StFl moiety to absorb the incident light, which results in reducing the PL intensity. The reversible structural change of the prepared ES fibers leads to an "on−off" PL intensity profile with temperature variation (Figure 7(C)).

Macroscopic Thermoresponsive Volume and Luminescence Variation of ES Fibers. Figure 9 shows the photographs of **P4** ES fiber mats immersed in deionized water as the temperature varied between 40 and 60 °C under visible light (Figure 9(A),(C)) and UV light (Figure 9(B),(D)). The ES fibers have their initial area and thickness of 3 cm^2 and 15 μm in the dry state, respectively, before immersing in water. As shown in images (A) and (C) in Figure 9, the area of the prepared ES fibers mat changes from 2.3 to 1.0 cm^2 as the temperature increases from 40 to 60 °C. It suggests that the ES fiber mat exhibits a rapid and significant shrinkage by 56 % of its initial area within 5 min. In addition, the PL intensity of the swollen mat at 40 °C is stronger than that of the shrunk mat at 60 °C under UV light illumination, as shown in images (B) and (D) in Figure 9, respectively. The rapid thermoresponsive luminescence or volume variation is due to the high surface/volume ratio of the ES fibers. The above results suggest the studied ES fibers

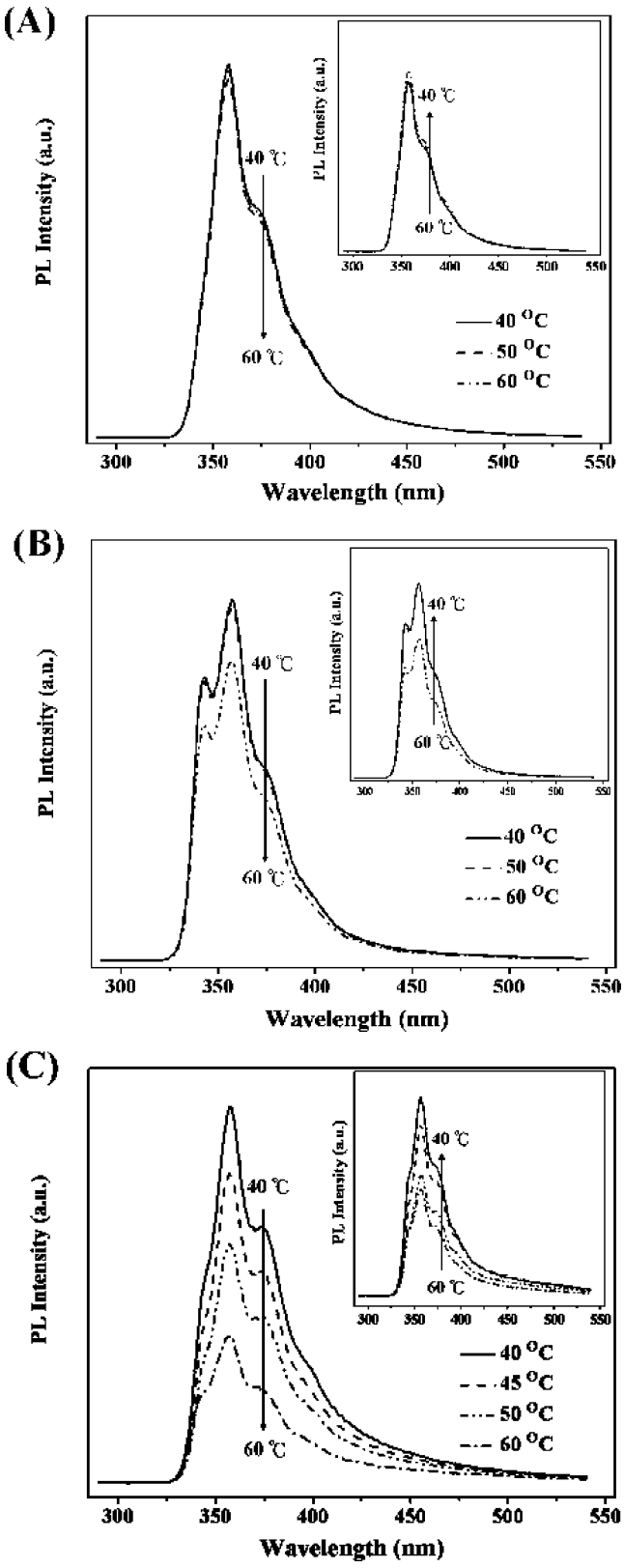

FIGURE 7. Photoluminescence spectra of poly(DMAEMA-*co*-SA-*co*-StFl) ES fibers in the temperature range of 40−60 °C: (A) P2, (B) P3, (C) P4. The inset figures are reverse process from 60 to 40 °C. (Note that all samples are excited at the wavelength of 290 nm.)

may have potential applications as multifunctional thermo-responsive sensory devices.

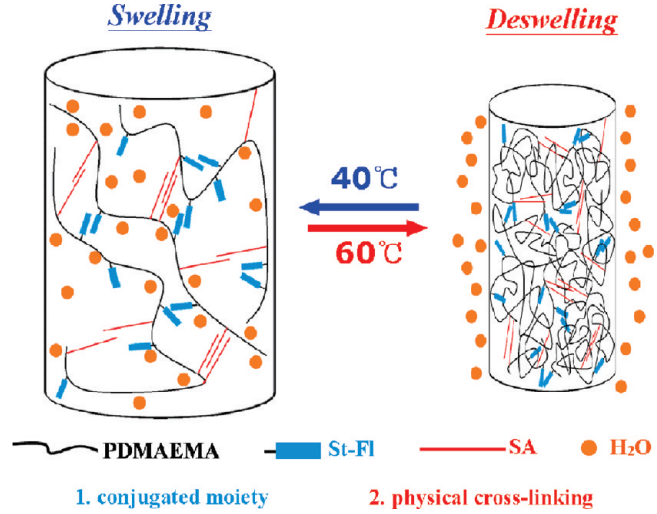

FIGURE 8. Schematic illustration of the morphological change for the P4 ES fibers soaked in water as the temperature heats up and cools down.

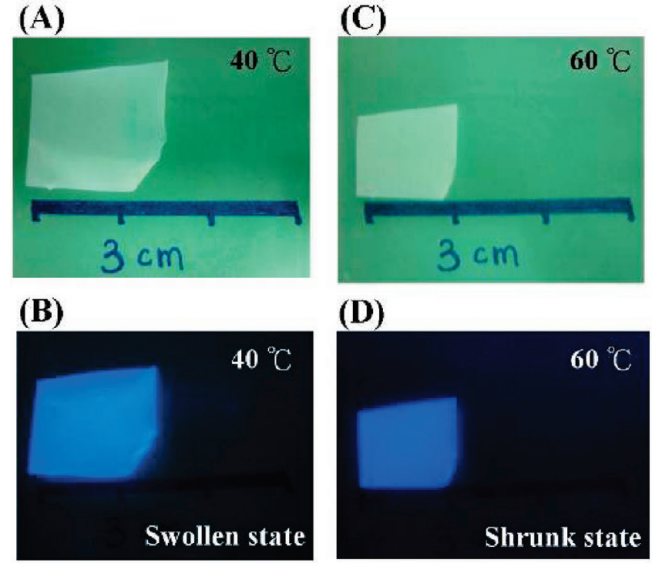

FIGURE 9. Optical images of P4 fiber mats in pure water at 40 and 60 °C: (A, C) under visible light, (B, D) under UV light.

CONCLUSIONS

Novel thermoresponsive luminescent ES fibers were successfully prepared by multifunctional poly(DMAEMA-*co*-SA-*co*-StFl) using a single-capillary spinneret. The prepared polymers of **P1**, **P3**, and **P4** showed the LCST of 40, 34, and 32.5 °C, respectively. It suggested the incorporating of the hydrophobic StFl and SA moieties reduced the polymer LCST. The diameters of the prepared **P2**−**P4** ES fibers estimated from FE-SEM were 200−1800, 400−800, and 600−800 nm, respectively. The more rigid structure of the StFl moiety probably resulted in an unstable cone-jet model through the ES process and led to the wide range of the prepared fibers. The **P4** ES fibers with the St-Fl aggregated domain size of 5−10 nm exhibited relatively an uniform blue emission under the UV illumination. A significant reversible photoluminescence quenching on the **P4** ES fibers was observed during the heating and cooling cycle. It was probably due to the light absorption ability of the StFl moiety

resulted from the extended/compact structural transformation on the PDMAEMA moiety. Furthermore, the high surface/volume ratio of the ES fibers led a much better temperature response on the fiber morphology compared with the corresponding spin-coated film. The present study demonstrated that the ES fibers prepared from multifunctional copolymers exhibited the thermoreversible variation on both volume and photoluminescence intensity.

Acknowledgment. The financial support from National Science Council of Taiwan, Ministry of Economics Affairs of Taiwan, and National Taiwan University Excellent Research program are highly appreciated.

Supporting Information Available: ^{1}H NMR spectra of **P1**, **P2**, and **P3** in CD_2Cl_2; TGA curves of **P1**, **P2**, **P3**, and **P4** copolymers copolymers at a heating rate of 10 °C/min under nitrogen atmosphere; DSC curves of **P1**, **P2**, **P3**, and **P4** copolymers at a heating rate of 10 °C/min under nitrogen atmosphere; FE-SEM images of **P1** ES fibers; FE-SEM images of the **P2** ES fibers treated by water with temperature at 20 °C; photoluminescence spectra of spin-coated film of **P4** in the temperature range of 40−60 °C (PDF). This material is available free of charge via the Internet at http://pubs.acs.org.

REFERENCES AND NOTES

(1) Liu, F.; Urban, M. W. *Prog. Polym. Sci.* **2010**, *35*, 3–23.
(2) Thomas III, S. W.; Joly, G. D.; Swager, T. M. *Chem. Rev.* **2007**, *107*, 1339–1386.
(3) Wolfbeis, O. S. *J. Mater. Chem.* **2005**, *15*, 3657–2669.
(4) Liu, C. L.; Lin, C. H.; Kuo, C. C.; Lin, S. T.; Chen, W. C. *Prog. Polym. Sci.* **2010**; DOI:10.1016/j.progpolymsci.2010 07.008, in press.
(5) Jenekhe, S. A.; Chen, X. L. *Science* **1998**, *279*, 1903–1907.
(6) Balamurugan, S. S.; Bantchev, G. B.; Yang, Y.; McCarley, R. L. *Angew. Chem., Int. Ed.* **2005**, *44*, 4872–4876.
(7) Xiao, X.; Fu, Y. Q.; Zhou, J. J.; Bo, Z. S.; Li, L.; Chan, C. M. *Macromol. Rapid Commun.* **2007**, *28*, 1003–1009.
(8) Yang, C. C.; Tian, Y.; Chen, C. Y.; Jen, A. K. Y.; Chen, W. C. *Macromol. Rapid Commun.* **2007**, *28*, 894–899.
(9) Tung, Y. C.; Wu, W. C.; Chen, W. C. *Macromol. Rapid Commun.* **2006**, *27*, 1838–1844.
(10) Wu, W. C.; Tian, Y.; Chen, C. Y.; Lee, C. S.; Sheng, Y. J.; Chen, W. C.; Jen, A. K. Y. *Langmuir* **2007**, *23*, 2805–2814.
(11) Li, C. S.; Wu, W. C.; Sheng, Y. J.; Chen, W. C. *J. Chem. Phys.* **2008**, *128*, 154908–154916.
(12) Lin, S. T.; Fuchise, K.; Chen, Y.; Sakai, R.; Satoh, T.; Kakuchi, T.; Chen, W. C. *Soft Matter* **2009**, *5*, 3761–3770.
(13) Lin, S. T.; Tung, Y. C.; Chen, W. C. *J. Mater. Chem.* **2008**, *18*, 3985–3992.
(14) Balamurugan, S. S.; Bantchev, G. B.; Yang, Y.; McCarley, R. L. *Angew. Chem., Int. Ed.* **2005**, *44*, 4872–4876.
(15) Ma, Z.; Qiang, L.; Zheng, Z.; Wang, Y.; Zhang, Z.; Huang, W. *J. Appl. Polym. Sci.* **2008**, *110*, 18–22.
(16) Iwai, K.; Matsumura, Y.; Uchiyama, S.; de Silva, A. P. *J. Mater. Chem.* **2005**, *15*, 2796–2800.
(17) Wang, D.; Miyamoto, R.; Shiraishi, Y.; Hirai, T. *Langmuir* **2009**, *25*, 13176–13182.
(18) Nagai, A.; Kokado, K.; Miyake, J.; Cyujo, Y. *J. Polym. Sci., Part A: Polym. Chem.* **2010**, *48*, 627–634.
(19) Muñoz-Bonilla, A.; Fernández-García, M.; Haddleton, D. M. *Soft Matter* **2007**, *3*, 725–731.
(20) Bougard, F.; Jeusette, M.; Mespouille, L.; Dubois, P.; Lazzaroni, R. *Langmuir* **2007**, *23*, 2339–2345.
(21) Li, J.; He, W. D.; Han, S.; Sun, X.; Li, L.; Zhang, B. *J. Polym. Sci., Polym. Chem.* **2009**, *47*, 786–796.
(22) Nakayama, M.; Okano, T. *Macromolecules* **2008**, *41*, 504–507.
(23) Zhang, Y.; Luo, S.; Liu, S. *Macromolecules* **2005**, *38*, 9813–9820.
(24) Lu, S.; Fan, Q. L.; Chua, S. J.; Huang, W. *Macromolecules* **2003**, *36*, 304–310.
(25) Gohy, J. F.; Creutz, S.; Garcia, M.; Mahltig, B.; Stamm, M.; Jerome, R. *Macromolecules* **2000**, *33*, 6378–6387.
(26) Lin, S.; Du, F.; Wang, Y.; Ji, S.; Liang, D.; Yu, L.; Li, Z. *Biomacromolecules* **2008**, *9*, 109–115.
(27) Jiang, T.; Chang, J.-B.; Wang, C.; Ding, Z.; Chen, J.; Zhang, J.; Kang, E.-T. *Biomacromolecules* **2007**, *8*, 1951–1957.
(28) Mingfeng, W.; Shan, Z.; Gerald, G.; Lei, S.; Kangqing, D.; Marcus, J.; Gilbert, C. W.; Gregory, D. S.; Mitchell, A. W. *Macromolecules* **2008**, *41*, 6993–7002.
(29) Reneker, D. H.; Chun, I. *Nanotechnology* **1996**, *7*, 216–223.
(30) Li, D.; Xia, Y. *Adv. Mater.* **2004**, *16*, 1151–1170.
(31) Chae, S. K.; Park, H.; Yoon, J.; Lee, C. H.; Ahn, D. J.; Kim, J. M. *Adv. Mater.* **2007**, *19*, 521–524.
(32) Babel, A.; Li, D.; Xia, Y.; Jenekhe, S. A. *Macromolecules* **2005**, *38*, 4705–4711.
(33) Kuo, C. C.; Lin, C. H.; Chen, W. C. *Macromolecules* **2007**, *40*, 6959–6966.
(34) Kuo, C. C.; Tung, Y. C.; Lin, C. H.; Chen, W. C. *Macromol. Rapid Commun.* **2008**, *29*, 1711–1715.
(35) Kuo, C. C.; Wang, C. T.; Chen, W. C. *Macromol. Mater. Eng.* **2008**, *293*, 999–1008.
(36) Wang, C. T.; Kuo, C. C.; Chen, H. C.; Chen, W. C. *Nanotechnology* **2009**, *20*, 375604.
(37) Kuo, C. C.; Tung, Y. C.; Chen, W. C. *Macromol. Rapid Commun.* **2010**, *31*, 65–70.
(38) Jabal, J. M. F.; McGarry, L.; Sobczyk, A.; Aston, D. E. *ACS Appl. Mater. Interfaces.* **2009**, *1*, 2325–2331.
(39) Fu, G. D.; Xu, L. Q.; Yao, F.; Li, G. L.; Kang, E. T. *ACS Appl. Mater. Interfaces* **2009**, *1*, 2424–2427.
(40) Tzeng, P.; Kuo, C. C.; Lin, S. T.; Chiu, Y. C.; Chen, W. C. *Macromol. Chem. Phys.* **2010**, *211*, 1048–1416.
(41) Wang, X.; Kim, Y. G.; Drew, C.; Ku, J.; Kumar, J.; Samuelson, L. A. *Nano Lett.* **2004**, *4*, 331–334.
(42) Wang, L.; Topham, P. D.; Mykhaylyk, O. O.; Howse, J. R.; Bras, W.; Jones, R. A. J.; Ryan, A. J. *Adv. Mater.* **2007**, *19*, 3544–3548.
(43) Yoon, J.; Chae, S. K.; Kim, J. M. *J. Am. Chem. Soc.* **2007**, *129*, 3038–3039.
(44) Kuo, C. C.; Wang, C. T.; Chen, W. C. *Macromol. Symp.* **2009**, *279*, 41–47.
(45) Davis, B. W.; Niamnont, N.; Hare, C. D.; Sukwattanasinitt, M.; Cheng, Q. *ACS Appl. Mater. Interfaces* **2010**, *2*, 1798–1803.
(46) Okuzaki, H.; Kobayashi, K.; Yan, H. *Macromolecules* **2009**, *42*, 5916–5918.
(47) Sugiyama, K.; Hirao, A.; Hsu, J. C.; Tung, Y. C.; Chen, W. C. *Macromolecules* **2009**, *42*, 4053–4062.
(48) Zhang, W.; Zhang, W.; Zhou, N.; Cheng, Z.; Zhu, J.; Zhu, X. *Polymer* **2008**, *49*, 4569–4575.
(49) Megelski, S.; Stephens, J. S.; Chase, J. B.; Rabolt, J. F. *Macromolecules* **2002**, *35*, 8456–8466.
(50) Osada, Y.; Matsuda, A. *Nature* **1995**, *376*, 219.

AM100760A